

Study on Dynamic Characteristics of Magnetic Suspending Flywheel Based on Finite Element Method

Hou Eryong^{1,a}, Liu Kun^{1,b}

¹Institute of Aerospace and Material Engineering, National University of Defense Technology, Changsha, 410073, China

^ahoueryong1@163.com, ^bliukun@nudt.edu.cn

Abstract: The configuration and principle of a magnetic suspending flywheel which was supported by hybrid magnetic bearings were introduced. A 3D finite element model of flywheel rotor was established by ANSYS10.0. The initial several vibration modes and frequencies were got in static state. The results of rigid vibration were compared with the theoretical ones, which proved the reasonability of the finite element model. The influence of radial and axial bearing stiffness and centrifugal prestress to dynamic characteristics was studied. The findings will be useful for the selection of control parameters and the optimization of the system.

Keywords: Magnetic Suspending Flywheel, Dynamic Characteristics, Finite Element Method, Bearing Stiffness, Centrifugal Prestress

1 Introduction

With the virtue of no mechanical abrasion, low power loss, high precision, long lifetime and the controllability of dynamic performance, magnetic suspending flywheel is the ideal actuator for attitude control system of spacecraft[1].

A hybrid magnetic suspending flywheel was designed, which has radial active controller and axial passive stability. The dynamic performance of magnetic suspending flywheel is determined by both the control system and the structural characteristics of magnetic bearing and rotor. Moreover, the vibration modes of flywheel affect its stability and control accuracy directly. So it is necessary to research the structural dynamic characteristics before control. Based on ANSYS10.0, the dynamic characteristics of our flywheel, including natural frequencies and mode shapes, were analyzed in this paper.

The flywheel is composite of outer stator and inner rotor as Fig.1. It contains two sets of radial bearings, the upper one and the lower one, and there is no axial bearing. Besides, the whole flywheel system contains driving motor, flywheel shell, underpan, auxiliary bearings, and sensors and so on. The magnetic bearings are divided into four symmetrical magnetic poles. The inner and outer radial of the rotor are 0.081m and 0.238m, respectively.

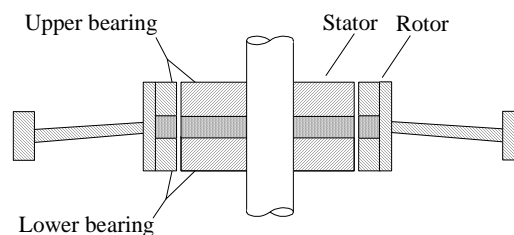


Fig.1 Configuration Sketch Map of the Hybrid Magnetic Suspending Flywheel

The stator of flywheel is fixed with the outside through the underpan and its bending

rigidity is far greater than the radial bearing stiffness and axial passive stabilization stiffness. The first order flexible natural frequency is about as twice as the rotor's. So the flexible deformation of stator can be neglected in the following calculation.

The magnetic bearings of flywheel work in the way of permanent magnet bias and electromagnet control, which can reduce the power loss of flywheel effectively. The swing and radial translation of rotor are controlled by electromagnetic windings. When the rotor translates axially, the magnetic field lines between the rotor and stator are distorted and the axial resilience is generated, and then the rotor suspends passively in axial direction.

2 Finite Element Model

The 3D finite element model of flywheel rotor was established in ANSYS10.0 with the origin of coordinates locating at the rotating axis and middle of the two bearings, as Fig.2. The mass of the rotor model is 2.7835kg. The center of mass is: $X_C=0$, $Y_C=0$ and $Z_C=0.0011\text{mm}$. Moments of inertia about center of mass are: $I_{XX}=I_{YY}=0.00847\text{kg}\cdot\text{m}^2$ and $I_{ZZ}=0.01522\text{kg}\cdot\text{m}^2$. The rotor is made of aluminum alloy, electric pure iron and stainless steel. All materials were taken as linear elastic ones according to the actual circumstance.

The magnetic bearings were simplified as springs and simulated with COMBINE14 element[2]. Every magnetic bearing was simplified as four symmetric springs in radial direction, as Fig.3. The passive stability in axial direction was simplified as eight springs, corresponding to the eight radial springs. All the stiffness coefficients of spring were determined by the controller and structure of bearing. One node of the element COMBINE14 was located at the inner wall of rotor, quartering points of the two bearing, and the other was constrained in radial and axial directions.

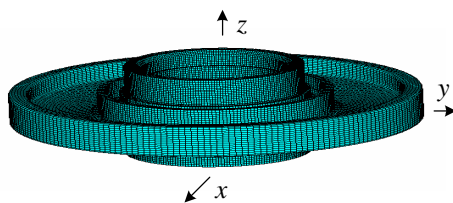


Fig.2 3D Finite Element Model of Rotor

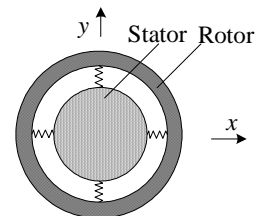


Fig.3 Sketch Map of Equivalent Bearing

3 Static Analysis

While rotating in high speed, the rotor will be deformed or destroyed due to centrifugal force. In order to validate the security of structure and the rationality of selection for material types, static analysis was carried out before the modal analysis. The angular velocity of rotor was within the range of zero to 13000rpm. The results show that the maximum von Mises stress and displacement vector sum of rotor are almost directly proportional to the square of its spin speed.

The distribution of the maximum von Mises stress and displacement vector sum were shown as Fig.5 with the spin velocity 13000rpm. The maximum von Mises stress is 138MPa at the nether root of turnplate. The maximum von Mises stress of LD10, 1Cr18Ni9Ti and DT4C are 138, 71.5 and 61.3 MPa respectively, which are less than their yield limit

correspondingly. Hence, the rotor is secure and the presumption of linear elastic for material is reasonable. The maximum displacement vector sum is 2.96mm at the outermost of flange.

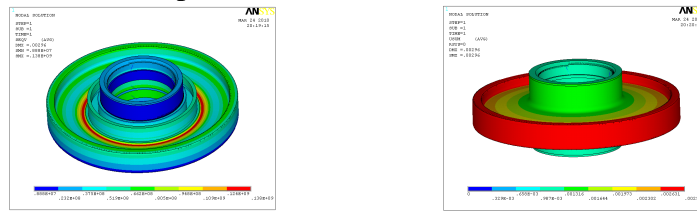


Fig.5 Distribution of the Maximum Von Mises Stress (left) and Displacement Vector Sum (right)
Corresponding to $\omega=13000\text{rpm}$

4 Modal Analysis

Taking no account of the spin velocity, the modal analysis was carried out in the method of Block Lanczos based on the above model. The initial several natural frequencies and corresponding mode shapes of rotor were got in static state as Tab.2. The first six orders are rigid modes and the others are flexible ones. Because the stiffness of bearing is far smaller than the rigidity of rotor itself, the low frequency vibration modes are mainly the rigid motion which includes rotation, swing, radial and axial translation of rotor relative to the stator and the high frequency vibration modes are the flexible deformation of rotor which includes bend, swing and axial translation of rotor plate relative to rotor hub. The rigid vibration modes are related to the bearing stiffness (stiffness coefficient of springs in finite element model), which is determined by the controller, structure of bearing and working state of flywheel. The rigid motion of rotor affects the control precision directly and should be restrained by proper methods. The flexible vibration modes are determined by the structural characteristics of rotor.

Tab.2 Natural Frequencies and Corresponding Vibration Modes
(Stiffness of flywheel in radial and axial directions are $K_x=4e5\text{N/m}$ and $K_z=3e5\text{N/m}$)

Order	Natural Frequency[Hz]	Vibration Mode
1	0	Rigid rotation about Z axis
2	28.323	Rigid swing about X axis
3	28.323	Rigid swing about Y axis
4	52.219	Axial rigid translation along Z axis
5	60.331	Radial rigid translation along X axis
6	60.331	Radial rigid translation along Y axis
7	1083.8	Rotor plate bending about X axis
8	1083.8	Rotor plate bending about Y axis
9	1404.3	Rotor plate swing about X axis relative to rotor hub
10	1404.3	Rotor plate swing about Y axis relative to rotor hub
11	1485.2	Rotor plate translation along Z axis relative to rotor hub
12	2918.4	Second order bending of rotor plate about X axis
13	2918.4	Second order bending of rotor plate about Y axis

Some typical vibration modes were shown as Fig.6. There are some pairs of coincident frequencies and vibration modes with a 90 degree discrepancy of phase because of the symmetrical structure and boundaries according as Tab.2. Therefore, only one of the same

modes is shown in Fig.6. Fig.6 (a) is rigid rotating mode owing to the free rotate of rotor about Z axis. Fig.6 (b) and (d) are rigid swing and radial translation modes owing to radial bearing stiffness. Fig.6 (c) is rigid axial translation mode owing to axial passive stability stiffness. The others are flexible vibration modes owing to structural characteristics of rotor itself.

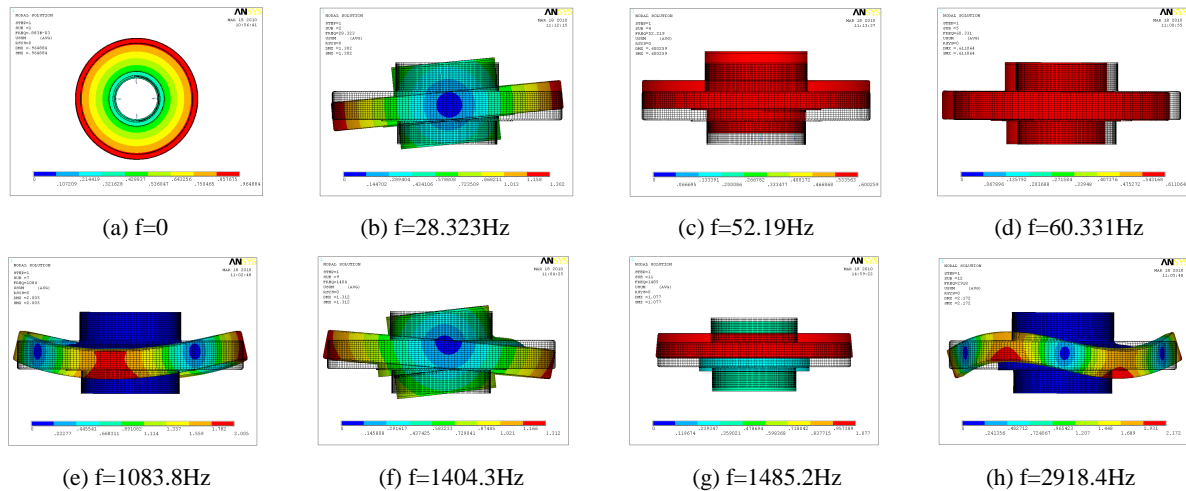


Fig.6 Typical Vibration Modes of Flywheel

In order to get the validity of finite element model, rigid natural frequencies were calculated through theoretical model which presumed that the rotor and stator were rigid bodies. The theoretical results were compared with the numerical ones as Tab.3 shown. The two results are in good agreement with each other with a 0.028% maximum relative error and the theoretical results are a little bigger than the numerical ones because of the presumption of rigid rotor. Thereby, the finite element model is rational and credible and can be used for further analysis.

Tab.3 Comparison of Rigid Natural Frequencies between Numerical and Theoretical Results

	Rigid Swing	Rigid Axial Translation	Rigid Radial Translation
Numerical Results[Hz]	28.323	52.190	60.331
Theoretical Results[Hz]	28.331	52.250	60.348
Relative Errors	-0.028%	-0.115%	-0.028%

4.1 Influence of Bearing Stiffness to Natural Frequency

The natural frequencies of system are related to radial bearing stiffness K_x as Tab.4 shown. Frequency A, C, E and H are independent of K_x , where frequency A is corresponding to the vibration mode of Fig.6(a), the others analogized in same manner. The influence to frequency G is tiny and can be neglected. Frequency B, D and F increase with K_x and the amplitude of B and D are notable. It is obvious that the variation of radial bearing stiffness mainly affects the frequencies of radial translation and swing, including rigid swing D and flexible swing F. But the influence to frequency F is not too serious because the stiffness is far smaller than the rigidity of rotor itself. The influence to frequency D which arises from radial bearing stiffness is notable by contraries.

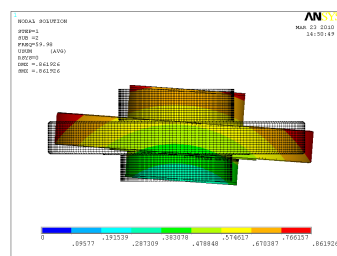
Tab.4 Natural Frequencies[Hz] Corresponding to Different Radial Bearing Stiffness ($K_z=3e5N/m$)

Kx[N/m]	4e5	4e6	1.2e7	4e7	1.7e8	1.8e8	2e8	4e8
a	0	0	0	0	0	0	0	0
b	28.323	37.463	52.120	84.115	153.15	156.54	162.88	206.32
c	52.219	52.219	52.219	52.219	52.219	52.219	52.219	52.219
d	60.331	190.16	327.03	582.66	1076.8	1098.6	1138.3	1328.3
e	1083.8	1083.8	1083.8	1083.8	1083.8	1083.8	1083.8	1083.8
f	1404.3	1404.9	1406.2	1411.0	1442.0	1445.4	1453.0	1582.4
g	1485.2	1485.2	1485.2	1485.3	1485.6	1485.6	1485.6	1485.9
h	2918.4	2918.4	2918.4	2918.4	2918.4	2918.4	2918.4	2918.4

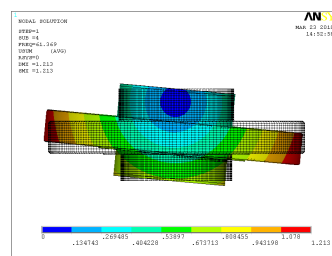
The natural frequencies of system are also related to axial bearing stiffness K_z as Tab.5 shown. Frequency A, E and H are independent of K_z . But frequency B, C, F and G increase with K_z and the amplitude of B and C are notable. The influence to frequency D is tiny and can be neglected. The variation of axial bearing stiffness mainly affects the frequencies of axial translation (including rigid axial translation B and flexible axial translation F) and swing (including rigid swing D and flexible swing F). In the same way, the influence to frequency F and G is not too serious. The influence to frequency C which arises from axial bearing stiffness is notable by contraries. While $K_z=1.5e6$ N/m, frequency B and D are greatly close to each other and their corresponding vibration modes are not pure swing or translation anymore but superposition of the two as Fig.7 shown, which is very disadvantage to the control of flywheel system.

Tab.5 Natural Frequencies[Hz] Corresponding to Different Axial Bearing Stiffness ($K_x=4e5$ N/m)

Kz[N/m]	0	3e5	4e5	1.2e6	1.5e6	3e6	8e6	2e7
a	0	0	0	0	0	0	0	0
b	8.2018	28.323	32.353	54.685	61.369	85.658	137.95	212.47
c	0	52.219	60.284	104.23	116.46	164.17	265.22	408.82
d	60.328	60.331	60.332	60.382	59.980	60.304	60.313	60.314
e	1083.8	1083.8	1083.8	1083.8	1083.8	1083.8	1083.8	1083.8
f	1404.0	1404.3	1404.5	1405.4	1405.7	1407.5	1413.3	1426.7
g	1484.8	1485.2	1485.3	1486.3	1486.7	1488.6	1494.8	1510.0
h	2918.4	2918.4	2918.4	2918.4	2918.4	2918.4	2918.4	2918.4



(a) $f=59.98$ Hz



(b) $f=61.369$ Hz

Fig.7 Some Vibration Modes of Flywheel ($K_x=4e5$ N/m, $K_z=1.5e6$ N/m)

4.2 Influence of Centrifugal Prestress to Natural Frequency

While the rotor rotates in high speed, its natural frequencies will be different from those in

static state due to centrifugal prestress. The influence of prestress can be deal with as a static problem by loading centrifugal inertial force which affects the rigidity of rotor directly[3]. In other words, rotation can cause stress stiffening of rotor. The add-in of stiffness due to stress stiffening will be added to the stiffness matrix to form a new one. In the case of prestressed modal analysis, the prestressed state of rotor is from an advance static analysis by using the PSTRES command[4].

In order to research the influence of centrifugal prestress to dynamic characteristics of flywheel, natural frequencies in different rotational speed were calculated and the results were shown in Tab.6. The vibration modes are the same as those in static state as Fig.6 shown. Frequency C and D are independent of prestress. But frequency A and B increase with rotational speed notably. Rigid rotation frequency A is equal to the spin frequency. Flexible natural frequencies increase with rotational speed slightly due to stress stiffening. Hence, centrifugal prestress mainly affects the frequencies of rigid swing and rotation.

Tab.6 Natural Frequencies[Hz] with Centrifugal Prestress Effect in Different Rotational Speed
 ($K_x=4e5$ N/m, $K_z=3e5$ N/m)

ω [rpm]	0	1000	3000	5000	6500	9000	11000	13000
a	0	16.667	50	83.333	108.28	150	183.33	216.67
b	28.323	32.429	55.152	83.941	106.49	144.99	176.08	207.32
c	52.219	52.219	52.219	52.219	52.219	52.219	52.219	52.219
d	60.331	60.332	60.389	60.302	60.309	60.313	60.314	60.314
e	1083.8	1084.2	1087.6	1094.3	1101.5	1117.5	1133.7	1152.9
f	1404.3	1404.6	1406.3	1409.8	1413.6	1422	1430.7	1441
g	1485.2	1485.3	1486.4	1488.4	1490.6	1495.6	1500.7	1506.8
h	2918.4	2918.7	2921.2	2926	2931.2	2942.9	2954.9	2969.2

5 Summary

In this paper, the dynamic characteristics of a hybrid magnetic suspending flywheel were analyzed by ANSYS10.0. It can be concluded that its low frequency vibration modes are mainly the rigid motion which includes rotation, swing, radial and axial translation of rotor relative to the stator and the high frequency vibration modes are the flexible deformation of rotor which includes bend, swing and axial translation of rotor plate relative to rotor hub. Natural frequencies of flywheel are related to the bearing stiffness, and the variation of bearing stiffness affects rigid natural frequencies notably but flexible ones slightly. The variation of radial bearing stiffness affects the frequencies of radial translation and swing. The variation of axial bearing stiffness affects the frequencies of axial translation and swing. Flexible natural frequencies and some rigid ones are increased in the case of centrifugal prestress and the amplitude increases with rotational speed. But the vibration modes are independent of centrifugal prestress.

The results provide a basis to the establishment of theoretical model and the design of structure and controller. Flexible natural frequencies can be changed by adjusting the structure or material type of rotor and the rigid ones can be changed by adjusting the parameters of controller or the structure of magnetic bearings. Then the natural frequencies

can be kept away from the working speed, which is indispensable to the flywheel.

References

- [1] Yongchun Xie. Control of active vibration for magnetic suspending momentum wheel[J]. Aerospace Control, 2001(2): 1-6.
- [2] Jingui Wan, Xiping Wang, Cuiyan Xia and etc. Finite element analysis on the dynamic characteristics of active magnetic bearing-rotor system[J]. Journal of Vibration and Shock, 2008, 27(S): 85-88.
- [3] Ronghua Su, Bijun Wang, Wenwen Ding and etc. Influence analysis of stress stiffening effect of rotating wheel-disc on its modal characteristics[J]. Journal of Engineering Design, 2009, 16(4): 293-296.
- [4] Release 10.0 documentation for ANSYS.